Proceedings of the 17th World Congress
The International Federation of Automatic Control
Seoul, Korea, July 6-11, 2008

Visual servo motion control of a spacecraft around an asteroid using feature points

Naoya Yanagi * **Fuyuto Terui** **

* *Graduate School of Information Systems, University of Electro-Communications, Tokyo, Japan (e-mail: ynaoya@chofu.jaxa.jp)*
** *Japan Aerospace Exploration Agency, Tokyo, Japan (e-mail: terui.fuyuto@jaxa.jp)*

Abstract: A visual servo motion controller is developed for maneuvering a planetary exploration spacecraft in proximity to an asteroid. The controller utilizes the positions of feature points in images of the asteroid taken by an onboard camera. These feature points are extracted from images using some metric and are directly fed back for the calculation of 6DOF control inputs (torque and force). The feasibility of the proposed control algorithm is investigated by a numerical simulation.

1. INTRODUCTION

Proximity maneuvers around an "uncooperative object" (target) are expected to be required for a variety of space missions, for example science missions such as the Japan Aerospace Exploration Agency's Hayabusa [1] (Fig. 1), which succeeded in touching down on the asteroid Itokawa in 2005, and on-orbit servicing and repair, such as the US Naval Research Laboratory's SUMO (Spacecraft for the Universal Modification of Orbits) [2], in which it is planned to capture an ordinary satellite in LEO (Low Earth Orbit) for operations such as orbit change, refuelling and repair.

Fig. 1. Asteroid "Itokawa" (actual image) and Hayabusa (CG).

This paper deals with the maneuver of a planetary exploration spacecraft in close proximity to an asteroid. At such distances, imaging sensors are supposed to play a fundamental role in guidance, navigation, and six degree-of-freedom (6DOF) control [Terui, 1998]. Since the target is non-cooperative, there is no communication with it, and no special markings or retro-reflectors on it to assist image processing [Terui *et al.*, 2006]. To address these problems, we adopt the technique of visual servo control. Visual servo control is originally an algorithm used for the motion control of a manipulator arm using images acquired from a camera mounted on the end-effector. This technique is widely used in practical situations such as object grasping or parts assembly in factory production lines. For more details about visual servo control, see [Hutchinson *et al.*, 1996] and [Chaumette and Hutchinson, 2006].

To apply this technique to 6DOF control in space, the controller utilizes the positions of feature points on the asteroid in images taken by a camera on board the spacecraft. These feature points could be existing surface areas with image texture, such as rocks and holes, or colored target markers released from the spacecraft to the surface of the asteroid. The feature points are expected to be extracted from images using some metrics and directly fed back for the calculation of 6DOF control inputs (torque and force).

As will be explained in section 2.1 in detail, since the image-based visual servo control algorithm is simple and intuitive, it is supposed to be able to design a 6DOF controller for a nonlinear plant which is robust against physical parameters such as mass and moment of inertia, and the properties of the actuators and camera calibration.

The remainder of this paper is organized as follows: In section 2, we present an overview of the visual servo control and introduce the image Jacobian for feature points. Then, we design a visual servo 6DOF controller using the dynamics of the translation and attitude motions of a spacecraft. In section 3, we investigate its feasibility by numerical simulation of flight in proximity to an asteroid.

2. VISUAL SERVO CONTROL

2.1 Overview of visual servo control

There are two categories of visual servo control method: image-based visual servo control (IBVS) and position-based visual servo control (PBVS). In IBVS, the desired

[1] `http://hayabusa.sci.isas.jaxa.jp`
[2] `http://projects.nrl.navy.mil/sumo`

value for the feedback control is a set of image features with values, and the motion of the camera is controlled by comparing the desired values with those of current image features. In other words, the motion of the camera is controlled by using the image of the target at the goal position. On the other hand, in PBVS the desired value for feedback control is the relative position and attitude of the target with respect to the camera. The motion of the camera is then controlled to the desired relative position and attitude using those given from the current image.

Since with IBVS there is no need to compute the relative position and attitude of the target, IBVS is faster than PBVS. PBVS is relevant to the problem of three-dimensional structure reconstruction, and the results of motion control are strongly influenced by camera calibration errors. For these reasons, we adopt IBVS in this thesis.

2.2 Derivation of image Jacobian for feature points

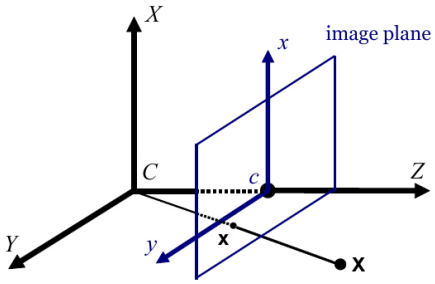

Fig. 2. Coordinate frames for the camera.

As shown in Fig. 2 we introduce the camera frame (X, Y, Z), which is set to be identical to the spacecraft's body-frame $\{b\}$, and the image plane (x, y). The origin of (X, Y, Z) is located at the optical center of camera, which coincides with the centroid of the spacecraft, and the Z-axis is aligned with the optical axis. The image plane (x, y) is perpendicular to the Z-axis with its origin at a distance of one unit length ahead from the origin of (X, Y, Z), for simplicity. The x-axis and y-axis are aligned parallel to the X-axis and Y-axis, respectively.

In this paper, we use feature points on the surface of an asteroid as a set of image features. A feature point $\mathbf{X} = (X, Y, Z)^\top$ expressed in the camera frame projects onto the image plane with image coordinates $\mathbf{x} = (x, y)^\top$. Let $\dot{\mathbf{f}} \in \mathcal{R}^k$ be the time derivative of the image coordinate vector for a set of feature points $\mathbf{f}$ with $k = 2n_f$, where n_f is the number of feature points, and let

$$\dot{\mathbf{r}} = (\mathbf{v}, \omega)^\top \tag{1}$$

be the motion rate of a spacecraft, with $\mathbf{v} \in \mathcal{R}^3$ the translational velocity of the origin of the spacecraft body-fixed reference frame $\{b\}$ and $\omega \in \mathcal{R}^3$ the angular velocity of $\{b\}$. The relationship between $\dot{\mathbf{f}}$ and $\dot{\mathbf{r}}$ is given by

$$\dot{\mathbf{f}} = \mathtt{J}\dot{\mathbf{r}} \tag{2}$$

where $\mathtt{J} \in \mathcal{R}^{k\times 6}$ is called the image Jacobian.

The image Jacobian is derived as follows. The relationship between $\mathbf{X} = (X, Y, Z)^\top$ and $\mathbf{x} = (x, y)^\top$ is

$$\begin{bmatrix} x \\ y \end{bmatrix} = \frac{1}{Z}\begin{bmatrix} X \\ Y \end{bmatrix}. \tag{3}$$

The time derivative of $\mathbf{X}$ is given by the well-known equation

$$\dot{\mathbf{X}} = -\mathbf{v} - \omega \times \mathbf{X}. \tag{4}$$

From (3) and (4), we obtain

$$\dot{\mathbf{x}} = \mathtt{J}\dot{\mathbf{r}} \tag{5}$$

where

$$\mathtt{J} = \begin{bmatrix} -\frac{1}{Z} & 0 & \frac{x}{Z} & xy & -(1+x^2) & y \\ 0 & -\frac{1}{Z} & \frac{y}{Z} & 1+y^2 & -xy & -x \end{bmatrix}. \tag{6}$$

Consider that one feature point in the image gives a constraint of two degrees-of-freedom. In order to determine the position and attitude of an object from image data, we need at least three feature points; that is, $k = 2n_f \geq 6$. For instance, when we have three feature points, $\mathbf{x}_1, \mathbf{x}_2, \mathbf{x}_3$, the vector of the image coordinates x_i, y_i $(i = 1, 2, 3)$ of the feature points set becomes

$$\mathbf{f} = (\mathbf{x}_1, \mathbf{x}_2, \mathbf{x}_3)^\top. \tag{7}$$

The image Jacobian in this case is

$$\mathtt{J} = \begin{bmatrix} \mathtt{J}_1 \\ \mathtt{J}_2 \\ \mathtt{J}_3 \end{bmatrix} \tag{8}$$

where $\mathtt{J}_i (i = 1, 2, 3)$ given by (6) corresponds to each set of feature points.

2.3 IBVS controller design for 6DOF control

The purpose of IBVS is to minimize the error defined by

$$\mathbf{e} = \mathbf{f}_g - \mathbf{f} \tag{9}$$

where $\mathbf{f}_g$ is the vector of the image coordinates of a set of feature points obtained at the goal position. In the following, we derive the control force and torque which minimize $\mathbf{e}$.

The equation of translational and attitude motion of a spacecraft is given by

$$m\dot{\mathbf{v}} = \mathbf{F} \tag{10}$$

$$\mathtt{I}\dot{\omega} + \omega \times \mathtt{I}\omega = \tau \tag{11}$$

where m is the spacecraft's mass, $\mathbf{F} \in \mathcal{R}^3$ is the applied force, $\mathtt{I} \in \mathcal{R}^{3\times 3}$ is the inertia matrix, and $\tau \in \mathcal{R}^3$ is the applied torque. Equations (10) and (11) are rewritten as

$$\mathtt{H}\ddot{\mathbf{r}} + \mathbf{h} = \mathbf{u} \tag{12}$$

where

$$\mathtt{H} = \begin{bmatrix} m & \mathbf{0}_{1\times 3} \\ \mathbf{0}_{3\times 1} & \mathtt{I} \end{bmatrix}, \mathbf{h} = \begin{bmatrix} \mathbf{0}_{3\times 1} \\ \omega \times \mathtt{I}\omega \end{bmatrix}, \mathbf{u} = \begin{bmatrix} \mathbf{F} \\ \tau \end{bmatrix}. \tag{13}$$

By differentiating (2), we obtain

$$\ddot{\mathbf{f}} = \dot{\mathtt{J}}\dot{\mathbf{r}} + \mathtt{J}\ddot{\mathbf{r}} \tag{14}$$

which is rewritten as

$$\ddot{\mathbf{r}} = \mathtt{J}^+(\ddot{\mathbf{f}} - \dot{\mathtt{J}}\dot{\mathbf{r}}) \tag{15}$$

where $\mathtt{J}^+ \in \mathcal{R}^{6\times k}$ represents the pseudo-inverse of $\mathtt{J}$.

Substituting (15) into (12), we obtain the dynamics of the feature points caused by the spacecraft's dynamics

$$\mathtt{HJ}^{+}(\ddot{\mathbf{f}} - \dot{\mathtt{J}}\dot{\mathbf{r}}) + \mathbf{h} = \mathbf{u}. \tag{16}$$

Here, we provide the dynamical behavior of error $\mathbf{e} = \mathbf{f}_g - \mathbf{f}$ such as

$$\ddot{\mathbf{f}} = \ddot{\mathbf{f}}_g + K_1(\dot{\mathbf{f}}_g - \dot{\mathbf{f}}) + K_2(\mathbf{f}_g - \mathbf{f}) \tag{17}$$

and by applying (17) to (16), we obtain the control input

$$\mathbf{u} = \mathtt{HJ}^{+}\left\{\ddot{\mathbf{f}}_g + K_1(\dot{\mathbf{f}}_g - \dot{\mathbf{f}}) + K_2(\mathbf{f}_g - \mathbf{f}) - \dot{\mathtt{J}}\dot{\mathbf{r}}\right\} + \mathbf{h}. \tag{18}$$

When the control input $\mathbf{u}$ given by (18) is substituted into (16), the closed loop dynamics of $\mathbf{e}$ becomes

$$\mathtt{HJ}^{+}(\ddot{\mathbf{e}} + K_1\dot{\mathbf{e}} + K_2\mathbf{e}) = \mathbf{0}. \tag{19}$$

Equation (19) shows that the error $\mathbf{e}$ converges to the zero with appropriate constant gains K_1 and K_2.

If we assume that the set of feature points obtained at the goal position is constant, that is $\dot{\mathbf{f}}_g = 0$, we finally obtain the force and torque control law

$$\mathbf{u} = \mathtt{HJ}^{+}\left\{-K_1\dot{\mathbf{f}} + K_2(\mathbf{f}_g - \mathbf{f}) - \dot{\mathtt{J}}\dot{\mathbf{r}}\right\} + \mathbf{h}. \tag{20}$$

Here $\dot{\mathbf{f}}$ is given by (2) and $\dot{\mathtt{J}}$ is calculated as

$$\dot{\mathtt{J}} = \frac{\mathtt{J}_k - \mathtt{J}_{k-1}}{\Delta t_i} \tag{21}$$

where k indicates the time step (iteration) and the image is updated at a regular interval Δt_i. ω could be obtained from a rate gyro, and $\mathbf{v}$ is obtained by integrating the output from an accelerometer.

3. NUMERICAL SIMULATION

We investigated the feasibility of the proposed algorithm by a numerical simulation. The target object is assumed to be an asteroid, and we used the three-dimensional model of the asteroid Itokawa (1998SF36) constructed from image data taken by Hayabusa. Itokawa measures approximately $535 \times 294 \times 209$ meters.

It is assumed that the asteroid is not moving with respect to the inertial frame $\{i\}$ with its origin fixed at the centroid of Itokawa, and three feature points on its surface with the $\{i\}$ frame coordinates $(160, 47, 71)$, $(-33, 137, 4)$, $(105, 73, -28)$ (meters) are extracted manually in advance of the maneuver based on following conditions:

a. The positions of the feature points on the 3D asteroid model in the goal image for the goal relative position/attitude are given in advance of the maneuver.
b. The feature points are extracted from images taken during the maneuver and their image coordinates are obtained.
c. Correspondence between the feature points in the goal image and the current image is ensured.
d. The total number of feature points is always 3; in other words, all feature points are always within the camera's field of view.
e. The depth Z of each feature point with respect to the camera frame is known, possibly by use of a laser range finder (LRF).

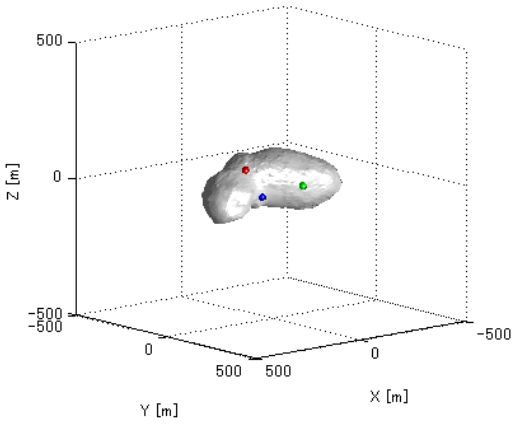

Fig. 3. The asteroid Itokawa and its feature points.

Table 1. Spacecraft Parameters.

mass (kg)	1000
inertia matrix (kg ·m^2)	$\begin{bmatrix} 1000 & 0 & 0 \\ 0 & 800 & 0 \\ 0 & 0 & 900 \end{bmatrix}$
start position (m)	(1000, 2000, -1000)
goal position (m)	(0, 600, 0)
initial translational velocity (m/s)	(0, 0, 0)
initial angular velocity (rad/s)	(0, 0, 0)

Table 2. Camera and LRF Specifications.

camera	focal length (mm)	10
	resolution (pixels)	640×480
	size of imaging device (mm)	6.4×4.8
LRF	resolution (m)	1

The simulation repeatedly carried out the following steps:

1. For each feature point in an image taken at the spacecraft's current position/attitude, compute its image coordinates in the image plane x, y and depth Z, then quantize these values according to the resolutions of the imaging device and the LRF.
2. Compute the control force and torque using (20).
3. Numerically integrate (10) and (11) and update the current position/attitude of the spacecraft.

The sampling time of the controller Δt_c is set to be 0.1 second and the image update interval Δt_i is assumed to be 1 second.

Table 1 shows the spacecraft's parameters, and the specifications of the camera and LRF are summarized in Table 2.

The results of the numerical simulation are shown in Figs. 4, 5 and 6. From Fig. 4, which shows the position of the spacecraft with respect to the inertia frame $\{i\}$, we can see that the spacecraft approaches the goal position. Fig. 5(b) shows that the error $\mathbf{e}$ decreases exponentially, as we expect from (19). From Fig. 5(a), it is noted that each feature point approaches its goal position in the image without going out of the field of view, and this is desirable. On the other hand, the spacecraft's trajectory in the inertial frame is indirect, and this could be improved.

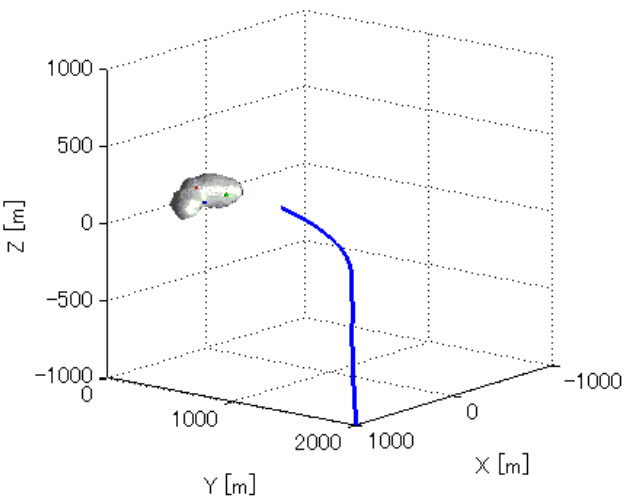

Fig. 4. Spacecraft approach trajectory (origin of $\{b\}$).

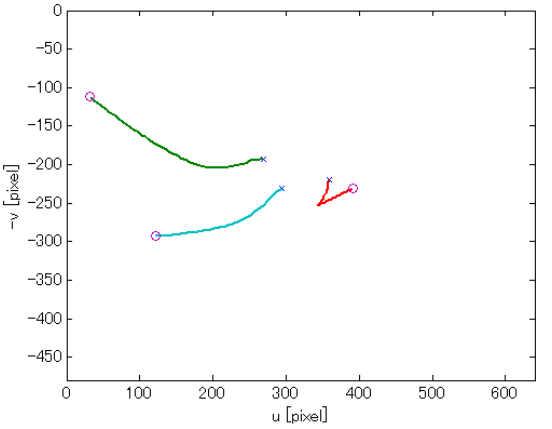

(a)

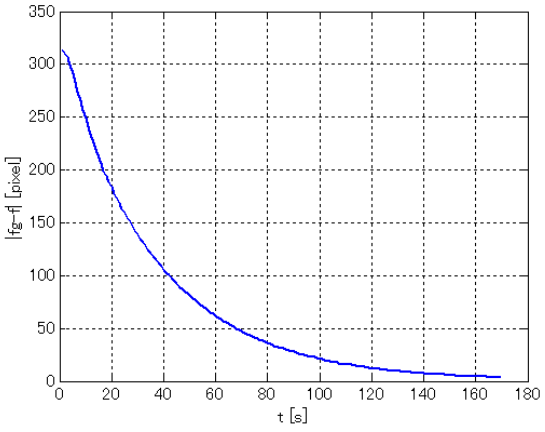

(b)

Fig. 5. (a) The loci of feature points during visual servo control. ×: feature points at the start position. ◯: feature points at the goal position. (b) Response of $|\mathbf{e}|$.

4. CONCLUSIONS AND FUTURE WORK

In this paper, we propose a visual servo motion controller for maneuvering a planetary exploration spacecraft in proximity to an asteroid. The controller uses feature points in an image as a source of the error signal and maps them directly to the control input. The results of a numerical simulation show that the proposed controller is feasible.

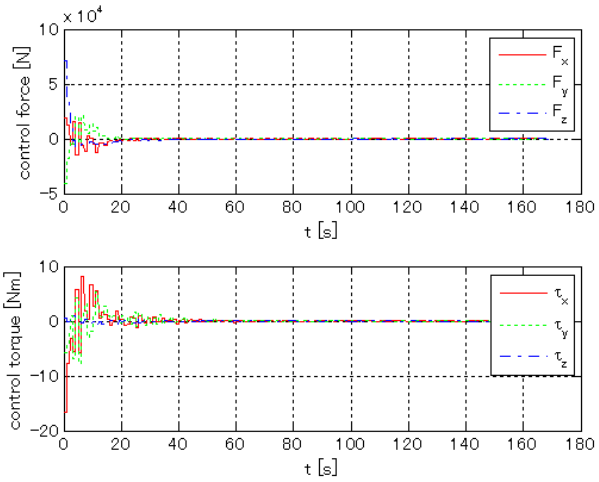

Fig. 6. $\mathbf{F}$ and τ versus time.

It is assumed in the simulation that the positions of feature points in the goal image are given *a priori* and these positions are always tracked in the image during the maneuver. Therefore, the extraction and tracking of the feature points during the maneuver could be a matter for further investigation. It is suspected that camera retreat caused by large camera axis rotation will be the problem that should be investigated. [Corke and Hutchinson, 2001]

ACKNOWLEDGEMENTS

The authors would like to thank Hayabusa science team for providing the three-dimensional model of Itokawa.

REFERENCES

F. Chaumette and S. Hutchinson (2006). Visual Servo Control Part I: Basic Approaches, *IEEE Robotics and Automation Magazine*, pages 82–90, December.

F. Terui (1998). Position and Attitude Control of a Spacecraft by Sliding Mode Control, *Proceedings of the American Control Conference*, pages 217–221.

F. Terui *et al.* (2006). Motion Estimation to a Failed Satellite on Orbit using Stereo Vision and 3D Model Matching, *International Conference on Control, Automation, Robotics and Vision (ICARCV)*, IEEE Catalog Number: 06EX1361C, ISBN: 1-4244-0342-1, Library of Congress: 2006923660.

S. Hutchinson, G. Hager and P. Corke (1996). A Tutorial on Visual Servo Control, *IEEE Transactions on Robotics and Automation*, 12:651–670.

P. Corke and S. Hutchinson (2001). A New Partitioned Approach to Image-Based Visual Servo Control, *IEEE Transactions on Robotics and Automation*, 17:507–515.